

Supramolecular Assembly on Surfaces: Manipulating Conductance in Noncovalently Modified Mesoscale Structures

Grace M. Credo,[†] Andrew K. Boal,[‡] Kanad Das,[‡] Trent H. Galow,[‡] Vincent M. Rotello,^{*,‡} Daniel L. Feldheim,^{*,†} and Christopher B. Gorman^{*,†}

Department of Chemistry, North Carolina State University, Raleigh, North Carolina 27695, and Department of Chemistry, University of Massachusetts, Amherst, Massachusetts 01003

Received April 25, 2002

Metal–molecule–metal junctions have been used to elucidate single-molecule properties in organic monolayers that are applicable in molecular electronics. For example, pore-based sandwich structures,^{1,2} mechanical break junctions,³ and Hg drop electrode top contacts^{4,5} have been used to characterize the current–voltage properties of organic monolayers. Studies have also employed scanning tunneling microscopy (STM)^{6,7} and conducting atomic force microscopy (cAFM)⁸ to probe the current–voltage properties of molecular junctions with more limited contact areas. In particular, reports of STM studies on redox-active molecular monolayers have described the use of electroactive moieties in molecular junctions to facilitate nonlinear current–voltage behavior.⁹ In a recent example, the nonlinear current–voltage phenomenon of negative differential resistance (NDR) was observed in an electroactive, ferrocene-terminated self-assembled monolayer (SAM).⁷ The identification of nonlinear current–voltage properties such as NDR for individual molecules expands the potential applicability of molecule-scale components from use as conductive wires to multistate molecular switches.^{2,5,10}

Chemical self-assembly is an attractive method for reversibly constructing well-defined supramolecular systems with properties defined by their molecular components.¹¹ In particular, hydrogen bonding is a familiar construction motif in natural systems and has been used to assemble functional nanostructures, such as metal nanoparticle-based networks.¹² Applying these concepts, noncovalent self-assembly provides a potential method to install and subsequently remove electroactive functionality in molecular electronics systems. To explore this possibility, we patterned a footprint region for molecular assembly on a surface featuring a recognition-element-terminated thiol. We then used moieties featuring complementary recognition to tune the current–voltage properties of the patterned region. In this work, we used an STM tip to pattern and probe molecular assemblies and independently verified the hydrogen bond-mediated assembly process using bulk electrochemical and spectroscopic techniques.

In our experiments, the initial “binder” molecule, diacyl 2,6-diaminopyridine decanethiolate (DAP, Figure 1A) was inserted into a background monolayer of decanethiolate on Au(111) using replacement lithography. As described in previous work,^{7,13} the desorption of the initial alkylthiolate SAM was induced by elevated tip bias voltages, and adsorption of the replacement thiolate from solution was conducted in a low dielectric solvent, such as dodecane. Electroactive functionalization of the monolayer was then achieved through binding of the complementary ferrocene-

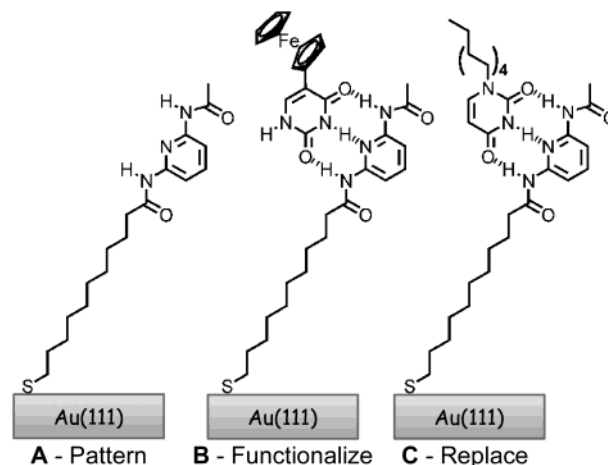


Figure 1. Formation of molecular assemblies. (A) Diacyl 2,6-diaminopyridine decanethiolate (DAP) “binder.” (B) Recognition of complementary electroactive ferrocene-uracil. (C) Recognition of complementary nonelectroactive dodecyl uracil “eraser.”

terminated uracil (Fc–uracil) to DAP (Figure 1B) by incubation of the sample in a Fc–uracil solution. Replacement of the electroactive Fc–uracil by a nonelectroactive dodecyl uracil (Figure 1C) “eraser” was effected by the exposure of the replacement region to a solution of dodecyl uracil.

Selections from a more extensive series of low-current STM (Digital Instruments E, Pt:Ir tips) images of noncovalent assembly on an initial mesostructure are shown in Figure 2 (see Supporting Information for more images). In the first row, the DAP replacement region (300 nm)² was imaged at several bias voltages (Figure 2A–C), as indicated. The current-dependent apparent height contrast in the same area after binding of the Fc–uracil increases at much lower bias voltages (0.3–1 V) relative to the DAP region alone (Figure 2D–F). The significant increase in apparent height contrast in the STM images is attributed to the electroactive Fc–uracil/DAP assembly (Figure 1B). This is consistent with STM imaging of patterned Fc-terminated alkylthiolates observed previously.^{7,13,14} STM images of the same region after exposure to dodecyl uracil (Figure 2G–I) indicated replacement of the electroactive Fc–uracil with the nonelectroactive dodecyl uracil as evidenced by the significant decrease in current-dependent apparent height contrast when compared to the DAP–uracil–Fc assembly region (Figure 2D–F). In Figure 2, the STM contrast in current–voltage properties among the different mesostructures becomes evident at bias voltages around 0.5 V (Figure 2B,E,H).

Recognition between the host–guest systems used in this study was further verified on nonpatterned assemblies by X-ray photoelectron spectroscopy (XPS, Figure 3A–C) and cyclic voltammetry

* To whom correspondence should be addressed. E-mail: chris_gorman@ncsu.edu; dan_feldheim@ncsu.edu; rotello@chem.umass.edu.

[†] North Carolina State University, Raleigh.

[‡] University of Massachusetts, Amherst.

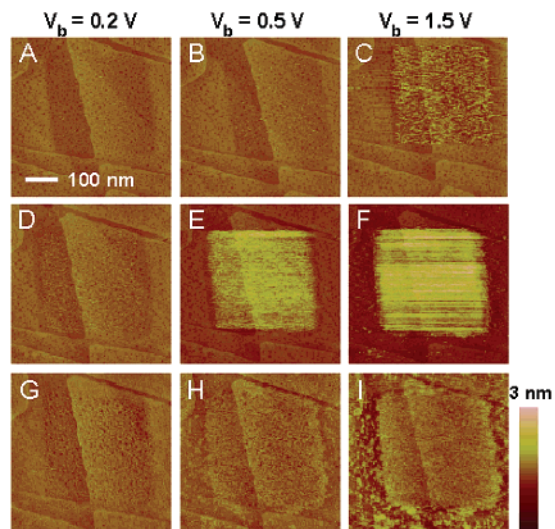


Figure 2. Low-current STM images of noncovalent assembly on a mesostructure footprint at several bias voltages (V_b), as labeled above. (A–C): Initial DAP replacement region inserted into a surrounding decanethiolate monolayer. (D–F): After binding of complementary electroactive Fc-uracil. (G–I): After binding of complementary dodecyl uracil. Setpoint current for all images was 10 pA.

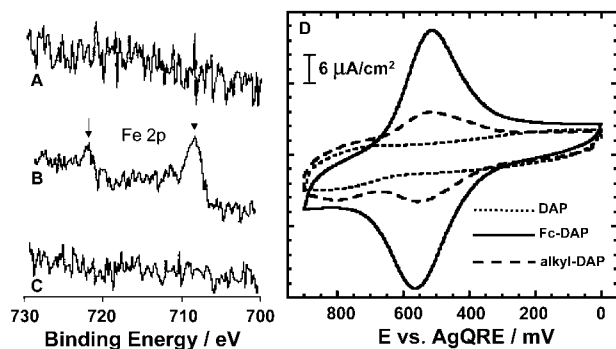


Figure 3. Bulk characterization of molecular assembly formation. XPS of (A) DAP monolayer, (B) Fc-uracil on DAP (708 and 722 eV peaks from Fe 2p), (C) iodo-labeled dodecyl uracil on DAP (iodine Auger peak at 733 eV, not shown) and (D) cyclic voltammograms (0.1 M TBAP in acetonitrile, Ag quasi-reference electrode, Pt counter, 100 mV/s, fourth cycle) of assembly.

(CV, Figure 3D). The peaks in Figure 3B at 708 and 722 eV are attributed to Fe (2p), confirming the presence of Fc-uracil on the surface. This peak disappeared with the replacement of Fc-uracil with iodo-labeled dodecyl uracil, concurrent with the appearance of the iodine Auger peak at 733 eV. Likewise, CV measurements indicated the binding of Fc-uracil to a DAP monolayer ($\Gamma = 5.3 \times 10^{-10}$ mol/cm²) and its subsequent replacement by dodecyl uracil (Figure 3D). Further discussion of DAP monolayer coverage and Fc-uracil binding is included in the Supporting Information section. The contrast in electrochemical current–voltage properties near 0.5 V in Figure 3D correlates with what was observed in Figure 2.

In summary, we have used complementary hydrogen bonding molecules to control the noncovalent self-assembly and electronic properties of a chemically well-defined surface mesostructure. Specifically, we have demonstrated the use of hydrogen bonding

to add and remove electroactive functionality in a mesoscale molecular assembly. In future studies, noncovalent interactions on a patterned surface can be used to construct increasingly complicated mesostructures with tunable current–voltage properties.

Acknowledgment. This research was supported by the Office of Naval Research (N00014-00-1-0633) and the National Science Foundation (CHE-9905492). Jacob Hirsch, Interface Analysis Lab Director, (Polymer Science and Engineering, U. Mass., Amherst) collected XPS of our samples. We thank Drew Wassel, Ryan Fuierer, and Young-Rae Hong (Chem., NCSU) for experimental assistance.

Supporting Information Available: Additional data (STM images and image analysis, XPS, CV), chemical syntheses, detailed experimental procedures (PDF). This material is available free of charge via the Internet at <http://pubs.acs.org>.

References

- (1) Chen, J.; Wang, W.; Reed, M. A.; Rawlett, A. M.; Price, D. W.; Tour, J. M. *Appl. Phys. Lett.* **2000**, *77*, 1224–1226.
- (2) Chen, J.; Reed, M. A.; Rawlett, A. M.; Tour, J. M. *Science* **1999**, *286*, 1550–1552.
- (3) Reed, M. A.; Zhou, C.; Muller, C. J.; Burgin, T. P.; Tour, J. M. *Science* **1997**, *278*, 252–254.
- (4) (a) Holmlin, E. E.; Haag, R.; Chabiny, M. L.; Ismagilov, R. F.; Cohen, A. E.; Rampi, M. A.; Terfort, A.; Whitesides, G. M. *J. Am. Chem. Soc.* **2001**, *123*, 5075–5085. (b) Holmlin, R. E.; Ismagilov, R. F.; Haag, R.; Mujica, V.; Ratner, M. A.; Rampi, M. A.; Whitesides, G. M. *Angew. Chem., Intl. Ed.* **2001**, *40*, 2316–2320.
- (5) Selzer, Y.; Salomon, A.; Ghabboun, J.; Cahen, D. *Angew. Chem., Intl. Ed.* **2002**, *41*, 827–830.
- (6) (a) Datta, S.; Tian, W.; Hong, S.; Reifenberger, R.; Henderson, J. I.; Kubiak, C. P. *Phys. Rev. Lett.* **1997**, *79*, 2530–2533. (b) Samanta, M. P.; Tian, W.; Datta, S.; Henderson, J. I.; Kubiak, C. P. *Phys. Rev. B* **1996**, *53*, R7626–R7629. (c) Tian, W.; Datta, S.; Hong, S.; Reifenberger, R.; Henderson, J. I.; Kubiak, C. P. *J. Chem. Phys.* **1998**, *109*, 2874–2882. (d) Xue, Y.; Datta, S.; Hong, S.; Reifenberger, R.; Henderson, J. I.; Kubiak, C. P. *Phys. Rev. B* **1999**, *59*, R7852–R7855. (e) Cui, X. D.; Primak, A.; Zarate, X.; Tomfohr, J.; Sankey, O. F.; Moore, A. L.; Moore, T. A.; Gust, D.; Harris, G.; Lindsay, S. M. *Science* **2001**, *294*, 571–574. (f) Gittins, D. I.; Bethell, D.; Schiffrin, D. J.; Nichols, R. J. *Nature* **2000**, *408*, 67–69. (g) Song, I. K.; Kaba, M. S.; Barteau, M. A. *Langmuir* **2002**, *18*, 2358–2362. (h) Donhauser, Z. J.; Mantooh, B. A.; Kelly, K. F.; Bunn, L. A.; Monnell, J. D.; Stapleton, J. J.; Price, D. W., Jr.; Rawlett, A. M.; Allara, D. L.; Tour, J. M.; Weiss, P. S. *Science* **2001**, *292*, 2303–2306. (i) Weiss, P. S.; Bumm, L. A.; Dunbar, T. D.; Burgin, T. P.; Tour, J. M.; Allara, D. L. *Ann. N.Y. Acad. Sci.* **1998**, *852*, 145–168.
- (7) Gorman, C. B.; Carroll, R. L.; Fuierer, R. R. *Langmuir* **2001**, *17*, 6923–6930.
- (8) (a) Zhao, J.; Uosaki, K. *Nano Lett.* **2002**, *2*, 137–140. (b) Wold, D. J.; Frisbie, C. D. *J. Am. Chem. Soc.* **2000**, *122*, 2970–2971. (c) Wold, D. J.; Frisbie, C. D. *J. Am. Chem. Soc.* **2001**, *123*, 5549–5556. (d) Wold, D. J.; Haag, R.; Rampi, M. A.; Frisbie, C. D. *J. Phys. Chem. B* **2002**, *106*, 2813–2816. (e) Ishida, T.; Mizutani, W.; Aya, Y.; Ogiso, H.; Sasaki, S.; Tokumoto, H. *J. Phys. Chem. B* **2002**, *106*, 5886–5892.
- (9) (a) Karzazi, Y.; Cornil, J.; Bredas, J. L. *J. Am. Chem. Soc.* **2001**, *123*, 10076–10084. (b) Tao, N. J. *Phys. Rev. Lett.* **1996**, *76*, 4066–4069. (c) Hipps, K. W.; Barlow, D. E.; Mazur, U. *J. Phys. Chem. B* **2000**, *104*, 2444–2447. (d) Scudiero, L.; Barlow, D. E.; Hipps, K. W. *J. Phys. Chem. B* **2000**, *104*, 11899–11905.
- (10) Sze, S. M. *Physics of Semiconductor Devices*, 2nd ed.; John Wiley & Sons: New York, 1981.
- (11) Reinhoudt, D. N.; Crego-Calama, M. *Science* **2002**, *295*, 2403–2405.
- (12) (a) Boal, A. K.; Ilhan, F.; DeRouchey, J. E.; Thurn-Albrecht, T.; Russell, T. P.; Rotello, V. M. *Nature* **2000**, *404*, 746–748. (b) Boal, A. K.; Galow, T. H.; Ilhan, F.; Rotello, V. M. *Adv. Funct. Mater.* **2001**, *11*, 461–465. (c) Boal, A. K.; Gray, M.; Ilhan, F.; Clavier, G. M.; Kapitzky, L.; Rotello, V. M. *Tetrahedron* **2002**, *58*, 765–770.
- (13) Fuierer, R. R.; Carroll, R. L.; Feldheim, D. L.; Gorman, C. B. *Adv. Mater.* **2002**, *14*, 154–157.
- (14) Gorman, C. B.; Carroll, R. L.; He, Y.; Tian, F.; Fuierer, R. *Langmuir* **2000**, *16*, 6312–6316.

JA0266823